

Effect of Atlantic Meridional Overturning Circulation on Tropical Atlantic Variability: A Regional Coupled Model Study

CAIHONG WEN

Wyle Information System/CPC, NCEP, NOAA, Camp Springs, Maryland

PING CHANG

Department of Oceanography, Texas A&M University, College Station, Texas, and State Key Laboratory of Satellite Ocean Environment Dynamics, Second Institute of Oceanography, Hang Zhou, Zhejiang, China

RAMALINGAM SARAVANAN

Department of Atmospheric Sciences, Texas A&M University, College Station, Texas

(Manuscript received 13 May 2010, in final form 26 November 2010)

ABSTRACT

A simplified coupled ocean–atmosphere model, where an atmospheric general circulation model (AGCM) is fully coupled to a 2½-layer reduced-gravity ocean model (RGO) over the tropical Atlantic basin, is presented in the context of studying the role of the Atlantic meridional overturning circulation (AMOC) in tropical Atlantic variability (TAV). In the ocean model, the strength of the AMOC is controlled by specifying mass transport at open boundaries. The fidelity of the reduced-physics model in capturing major features of tropical Atlantic variability, as well as its response to the AMOC changes, is demonstrated in a series of model experiments. The results of the experiments reveal the relative importance of oceanic processes and atmospheric processes in AMOC-induced tropical Atlantic variability–change. It is found that the oceanic processes are a primary factor contributing to the warming at and south of the equator and the precipitation increase over the Gulf of Guinea, while atmospheric processes are responsible for the surface cooling of the tropical North Atlantic and southward displacement of ITCZ.

A systematic investigation of the coupled system response to changes in AMOC strength indicates that the SST over the cold-tongue region responds nonlinearly to AMOC changes. The sensitivity of the SST response increases rapidly when AMOC strength decreases below a threshold value. Such nonlinear behavior is also found in precipitation response over the Gulf of Guinea. These results suggest that complex and competing atmosphere–ocean processes are involved in TAV response to AMOC changes and the nature of the response can vary from one region to another. This complexity should be taken into consideration in Atlantic abrupt climate studies.

1. Introduction

The Atlantic meridional overturning circulation (AMOC) is one of the most prominent ocean circulation systems. It is responsible for the northward heat transport at all latitudes within the Atlantic Ocean. Because of its potentially important role in abrupt climate change, observing and understanding of the AMOC have been a major research focus in recent years. Paleo-proxy records

indicate a strong relation between rapid AMOC changes and global-scale abrupt climate changes during glacial and interglacial periods (e.g., Broecker et al. 1985; Haug et al. 2001; Piotrowski et al. 2005). Rapid changes in hydrological cycle of the North Atlantic have been postulated as a driver of the significant weakening or even a shutdown of AMOC (Broecker et al. 1985). This hypothesis has prompted the popular use of the so-called water-hosing experiments to simulate the weakening of AMOC and to study its impact on global climate.

Multimodel water-hosing experiments reveal certain robust response features of tropical Atlantic to a weakened AMOC, which includes a dipole-like SST pattern with cooler (warmer) temperature over the north (south)

Corresponding author address: Caihong Wen, Room 605-A, WWB, 5200 Auth Rd., NOAA/NWS/NCEP/Climate Prediction Center, Camp Springs, MD 20746.
E-mail: caihong.wen@noaa.gov

tropical Atlantic, a C-shaped cross-equatorial flow near the surface of the atmosphere and a southward shift of the intertropical convergence zone (ITCZ) (e.g., Stouffer et al. 2006; Timmermann et al. 2007; Zhang and Delworth 2005). The robustness of the responses indicates that there exists a tight linkage between AMOC changes and tropical Atlantic climate. Yet the detailed mechanisms by which the AMOC exerts its influence on TAV remain to be elucidated.

Recent studies suggest that both oceanic and atmospheric processes contribute to the influence of the AMOC on TAV. For oceanic processes, a frequently invoked mechanism is that AMOC changes modulate interhemispheric heat transport through planetary wave adjustment, which in turn affects the cross-equatorial SST gradient (Yang 1999; Johnson and Marshall 2002). Recently, Chang et al. (2008, hereafter referred to as C08) put forward a different mechanism, in which it was conjectured that a substantially weakened AMOC can trigger a tropical SST response by modifying the pathway of the subtropical cells (STCs). This hypothesis was tested by Wen et al. (2010, hereafter referred to as W10), who performed extensive sensitivity experiments using a 2½ reduced-gravity ocean model (RGO) model to examine the mechanism proposed by C08 in detail. They showed that the warming in the Gulf of Guinea and off the coast of Africa is linked to the reversal of the direction of the North Brazil Current (NBC) caused by the weakening of the AMOC, thereby supporting the oceanic teleconnection mechanism proposed by C08. For atmospheric processes, Chiang and Bitz (2005, hereafter referred to as CB05) suggested that a cooling in the high latitudes could be readily transmitted to the tropics through the wind–evaporation–SST (WES) feedback. This mechanism operates through intensifying northeasterly trade winds that leads to an increase in the latent heat loss and a cooling in the north tropical Atlantic, resulting in a southward shift of ITCZ. In a follow-up study, Chiang et al. (2008) showed that the WES feedback plays a more important role than the oceanic dynamical adjustment in the equatorward progression of SST anomalies induced by the weakening of AMOC. By limiting air–sea coupling in certain key areas in coupled GCM experiments, Krebs and Timmermann (2007) and Wu et al. (2008) suggested that ocean dynamical adjustments account for warming in the Southern Hemisphere, while the atmospheric teleconnection contributes the equatorward spreading North Atlantic cool SST anomalies and the shift of ITCZ.

Although these recent studies have shed light on the teleconnection mechanisms linking changes in the high-latitude North Atlantic to the tropics, more detailed studies are needed to fully explore the sensitivity of

tropical Atlantic climate response to AMOC changes. This is because atmospheric and oceanic processes may exert a competing influence on the tropical Atlantic response, and thus it is important to sort out how the net response is controlled by these competing processes and how it varies geographically. As pointed out by Chiang et al. (2008), the ocean adjustment tends to counter surface cooling in the North Atlantic by warming up subsurface temperature. Wan et al. (2009) show that the competing atmospheric and oceanic processes give rise to a complex response of the Caribbean SST to AMOC changes. Zhang (2008) also highlight the importance of atmospheric-induced surface cooling and oceanic-induced subsurface warming in the Atlantic decadal variability associated with the AMOC.

Using an ocean-only model, W10 show that a shutdown of AMOC induces surface warming in the entire tropical Atlantic. It suggests that the ocean dynamics alone cannot explain the dipole-like SST pattern associated with AMOC changes. Thus, to fully explain the response of tropical Atlantic to AMOC changes, it is necessary to consider contributions of both oceanic and atmospheric processes. For this, we need a coupled ocean–atmosphere model. Although fully coupled global circulation models (CGCMs) provide the most comprehensive simulations of climate variability–change, it can be difficult to clearly identify crucial dynamics from these models owing to complexities of coupled air–sea interactions and teleconnection mechanisms. Therefore, it is sometimes useful to use a reduced-physics climate model to examine the underlying dynamical processes. In this study, we present such a model. The new model is a regional coupled model (RCM), which couples the 2½-layer RGO model over the tropical Atlantic basin used in W10 to an atmospheric general circulation model (AGCM). The model not only has the advantage of computational efficiency that permits a large number of sensitivity experiments, but it also includes a number of novel features that are well suited for examining the relative importance of oceanic and atmospheric teleconnections. For example, the return limb of the AMOC can be controlled directly by varying the mass transport at the open boundaries of the ocean model, as demonstrated in W10. The use of a regional coupling strategy also allows for an effective separation of AMOC's influence on tropical Atlantic variability (TAV) from other remote influences, such as the El Niño–Southern Oscillation (ENSO). By forcing the atmosphere and ocean model independently, we can further isolate the effect of atmospheric processes on TAV from that of oceanic processes. Moreover, the simplified ocean dynamics make it easier and more straightforward in diagnosing relevant dynamical processes.

The main objective of this study is to elucidate the relative importance of the atmospheric processes proposed by CB05 versus the oceanic processes proposed by C08 in AMOC-induced TAV change. Note that the TAV in this study only refers to the seasonal variability of the tropical Atlantic climate. In particular, we will focus on two specific scientific questions.

First, what is the role of the oceanic and atmospheric processes in affecting the annual cycle of the Atlantic cold-tongue–ITCZ complex (Mitchell and Wallace 1992)? Coupled model experiments show that a shutdown of the AMOC has a significant impact not only on the climatological mean state of SST but also on the equatorial SST seasonal cycle with the strongest change occurring during boreal summer and fall (Wu et al. 2008; C08; Haarsma et al. 2008). Both oceanic dynamics and atmospheric processes may contribute to the marked seasonal response of SST to AMOC change. The former has been tested in an ocean-alone model (W10). The latter, however, has not been fully explored. It is widely recognized that there is a close linkage between tropical Atlantic SST and rainfall variability over the Nordeste region of Brazil and the Sahel region of West Africa based on numerous observational and modeling studies (Moura and Shukla 1981; Hastenrath 1984; Nobre and Shukla 1996; Fontaine et al. 1999). A question we will address in this study is how changes in the SST seasonal cycle induced by AMOC changes affect the seasonal variation of the precipitation in the regions. We will conduct numerical experiments to investigate the annual cycle response of the SST and associated rainfall of the tropical Atlantic to a shutdown of the AMOC and the relative role of atmospheric and oceanic processes in this response.

Second, what is the role of oceanic and atmospheric processes in determining the behavior of the SST response to changes in the AMOC? Sensitivity experiments of W10 show that tropical Atlantic SST response to AMOC changes behaves nonlinearly in the ocean-alone model. The warming rate of the SST increases dramatically when the AMOC strength falls below a threshold value of about 8 Sv (1 Sv $\equiv 10^6 \text{ m}^3 \text{ s}^{-1}$), at which the equatorward transport carried by the northern STC is approximately equal to the northward transport carried by the NBC. The study, however, did not take into consideration ocean–atmosphere feedbacks and atmospheric processes. It is not clear whether the nonlinear behavior of the SST response will hold in a coupled system. Therefore, in this study we will conduct sensitivity experiments using the coupled model to investigate the behavior of the SST response and the associated atmospheric response in the tropical Atlantic by varying AMOC strength systematically.

The paper is organized as follows. Section 2 provides an introduction of the coupled model and a description of numerical experiment design. Section 3 gives an evaluation of model simulation of tropical Atlantic climate. Section 4 discusses the influence of AMOC change on tropical Atlantic climate and relative contribution of atmospheric and oceanic processes. In section 5, we examine the sensitivity of the tropical Atlantic response to changes in the AMOC. Our major results will be summarized and discussed in section 6.

2. An Atlantic RCM and experiment design

The atmospheric component, AGCM, of the RCM used in this study is the Community Climate Model version 3.6.6 (CCM3) developed at the National Center for Atmospheric Research (NCAR). The horizontal resolution of the AGCM used in this study is the standard resolution T42 (triangular spectral truncation at wavenumber 42, corresponding to a grid resolution of about $2.8^\circ \times 2.8^\circ$ in the tropics). It has been shown that the CCM3 is able to capture the major global-scale features of atmospheric circulations (Hurrell et al. 1998) and reproduce a fairly realistic atmospheric response to SST variability in tropical Atlantic sector (Saravanan and Chang 2000; Chang et al. 2000).

The oceanic component of the RCM is the 2½-layer RGO model described in W10. This model consists of two active layers, the mixed layer and the thermocline layer. The infinitely deep water below the thermocline layer is assumed to be motionless, resulting in a reduced-gravity ocean. The governing equations of this model are described in detail in W10. Here, we only give a brief description of the thermodynamic equations in the RGO:

$$\begin{aligned} \frac{\partial T_1}{\partial t} + \frac{u_1}{a \cos \theta} \frac{\partial T_1}{\partial \phi} + \frac{v_1}{a} \frac{\partial T_1}{\partial \theta} \\ = \frac{Q_0 - Q_{-h_1}}{\rho_1 C_p h_1} - \frac{\omega H(\omega)}{h_1} (T_1 - T_2) \\ + K_t \nabla^2 T_1 + K_z \frac{\partial^2 T_1}{\partial z^2}, \quad \text{and} \end{aligned} \quad (1)$$

$$\begin{aligned} \frac{\partial T_2}{\partial t} + \frac{u_2}{a \cos \theta} \frac{\partial T_2}{\partial \phi} + \frac{v_2}{a} \frac{\partial T_2}{\partial \theta} \\ = \frac{Q_{-h_1}}{\rho_2 C_p h_2} + Q_{\text{cre}} - \frac{\omega H(-\omega)}{h_2} (T_1 - T_2) \\ + K_t \nabla^2 T_2 + K_z \frac{\partial^2 T_2}{\partial z^2}, \end{aligned} \quad (2)$$

where T_1 and T_2 are the temperature in the mixed layer and the thermocline layer, u_i (v_i) are the zonal (meridional)

components of velocity for layer i , and h_i is the thickness of layer i . Here, Q_o and Q_{-h1} are the downward net heat flux at the surface and the downward heat flux at the base of the mixed layer. A key aspect of the C08 oceanic mechanism is the water mass exchange between the warmer and saltier of northern subtropical gyre water and the cooler and fresher tropical gyre water. To include this important process in our simple model, we adopt a simple approach to maintain an idealized temperature front in the thermocline layer by adding a specified heat source term Q_{cre} in the thermocline temperature equation. Here, ω is the total exchange rate of water mass across the base of the mixed layer, it is calculated according to McCreary et al. (1993); C_p is specific heat of water; K_t and K_z are the horizontal and vertical heat diffusion coefficient, respectively; and $H(x)$ is the Heaviside step function [$H(x) = 1$ if $x \geq 0$; $H(x) = 0$ if $x < 0$]. The RGO covers the tropical Atlantic basin from 30°S to 30°N and 100°W to 20°E with realistic coastal lines. The northern and southern boundaries are open. Following the formulation by Marchesiello et al. (2001), open boundary conditions (OBCs) are utilized along the northern and southern boundaries. One advantage of using OBCs is that the strength of AMOC can be altered by modifying the northward mass transport at the open boundaries. W10 demonstrated that the RGO was able to reproduce major salient features of circulation in the upper tropical Atlantic when it was driven by observed surface forcing. The interested readers are referred to the appendix of W10 for a more detailed description of the model, including the complete model equations.

The CCM3 is fully coupled to the RGO within the tropical Atlantic from 30°S to 30°N without flux correction. The CCM3 exchanges surface fluxes with the RGO once per day, at which the daily mean surface heat fluxes and wind stresses from the CCM3 are provided to the RGO, while the simulated SST from the RGO is supplied to the CCM3. Outside of the tropical Atlantic (30°S to 30°N), observed annual cycle of SST is prescribed for the CCM3.

As aforementioned, the primary objective of this study is to identify the relative contribution of the atmospheric and oceanic processes to the responses of tropical Atlantic to AMOC changes. A way of assessing these contributions from these processes is to conduct a suite of experiments where only one or both teleconnection mechanisms are present. The following is a brief description of the experiments conducted in this study.

Control (CTRL) run: A 14-Sv mass transport is specified at the northern open boundary of the oceanic component to mimic the return flow of the AMOC. This run forced by a “realistic” combination of winds and the

AMOC represents “the current climate state.” We use this simulation as a reference for other sensitivity experiments. The experiment consists of a 120-yr single integration and the simulation approaches an equilibrium state after about 10-yr of integration. The model climatology and variability are derived from the last 80 years of simulation.

Ocean mechanism experiment (OME): This simulation is the same as the CTRL run except that the northward mass transport at the open boundaries of the oceanic component is set to zero, representing a climate state when the AMOC is shutdown completely. Since no other external forcing is present in the model, the difference between this and the CTRL run should only be attributed to the shutdown of the AMOC. Thus, this experiment allows us to examine the extent to which the oceanic processes and coupled feedbacks contribute to the TAV response to a shutdown of the AMOC.

Atmospheric mechanism experiment (AME): In this experiment, the RGO is forced by a negative surface heat flux anomaly derived from an ensemble of Geophysical Fluid Dynamics Laboratory Climate Model version 2.1 GFDL (GFDL CM2.1) water-hosing runs (Zhang and Delworth 2005) between 10° and 30°N. The rest of the model configuration is identical to that of the CTRL run. Since the AMOC return flow is kept at the same value as the CTRL run, this experiment allows us to test the effect of AMOC-induced cooling in the North Atlantic on TAV via the atmospheric processes.

Oceanic-atmospheric mechanism experiment (OAME): In this experiment, the northward mass transport at the open boundaries of the oceanic component is set to 0 as in the OME and the heat flux anomaly is applied to the RGO between 10° and 30°N as in the AME. Since both forcings are used simultaneously, this experiment is designed to assess the combined effect of oceanic and atmospheric processes on the TAV response to AMOC changes.

It is worth pointing out that in a fully coupled model water-hosing experiment, the surface cooling in the high-latitude North Atlantic occurs together with the weakening of the AMOC. Both the surface cooling and the AMOC change can affect TAV. In our experiments, we artificially separate these effects to evaluate their relative contribution to TAV. One may argue this separation is dynamically inconsistent, but we believe this is necessary to gain a better understanding of each process.

The above-described three sensitivity experiments start from the same equilibrium state of the CTRL run at year 10. Each consists of an 80-yr integration. All the analyses shown below are based on the last 65 yr of the 80-yr integration. Unless stated otherwise, anomalies of each experiment are referred to as the difference between the corresponding sensitivity run and the CTRL

run. Before proceeding to the discussion of the sensitivity runs, we first evaluate the simulated mean climate and climate variability of tropical Atlantic in the CTRL integration.

3. Simulated Atlantic mean climate

In this section, we will evaluate the performance of the model by comparing the simulated Atlantic mean climate in the CTRL run with observations. We will examine the annual mean state and the seasonal cycle, as the latter is a dominant atmosphere–ocean coupled signal in the tropical Atlantic.

Figure 1 shows the simulated and observed annual mean state of SST, surface wind stresses, and precipitation. The RCM captures gross features of the observed mean climate state, though with some apparent error in certain areas. Compared with the Reynolds SST analysis (Smith et al. 1996), the model underestimates the annual mean SST over most of the tropical Atlantic basin by about 1°C except that an excessive warm bias is found along the coast of Angola with a maximum error of 3°C. This infamous warm bias has been identified as a common problem for nearly all fully coupled GCMs (Davey et al. 2002; Breugem et al. 2006). Many hypotheses have been put forward to explain the cause of this warm bias, such as insufficient amount of stratus cloud in the region (e.g., Ma et al. 1996; Yu and Mechoso 1999) and inadequate representation of vertical mixing in the ocean (Hazeleger and Haarsma 2005). Our sensitive studies show that the magnitude of the warm bias is sensitive to the strength of the entrainment rate at the base of oceanic mixed layer (not shown). It suggests that an underestimation of coastal upwelling may be a major contributing factor for the warm bias in our model, although the lack of a realistic representation of the Atlantic stratus deck in the model can be also a major factor. The simulated southeast trade wind in the model is weaker than the wind in the National Centers for Environmental Prediction (NCEP) reanalysis (Kalnay et al. 1996) from the equator to around 15°S, located north of the warm SST bias. The intensity and location of the ITCZ is reasonably well simulated in comparison with the observation from the Global Precipitation Climatology Project (GPCP) (Huffman et al. 1997), although the heavy precipitation band over the ocean spreads too far southward along the Brazilian coast, giving an appearance of a “double ITCZ.” In the observation, the vertical thermal structure along the equator is characterized by a well-defined thermocline separating colder deep water from warmer surface water. The thermocline shoals eastward in response to the prevailing trade winds (Fig. 2b). Since the RGO only consists of two active layers, that is, a mixed layer

(upper layer) and thermocline layer (lower layer), the actual thermocline lies within the thermocline layer and its structure can be approximated by the mixed layer depth. As shown in Fig. 2a, the depth and the west-to-east tilt of the thermocline are reasonably captured by the RGO model.

One of the most prominent features of Atlantic climate variability is the pronounced annual cycle of cold tongue. Figure 2c depicts the seasonal cycle of simulated SST (contour) and entrainment velocity at the base of the mixed layer (shaded) along the equator. Both the simulated amplitude and phase of SST agree well with the observation shown in Fig. 2d, except that the simulated cold-tongue variation is located to the west of the observed variation and lags the observation by about 1 month owing to the delayed development of the vertical entrainment at the base of the mixed layer.

Figure 3 compares the observed precipitation and NCEP reanalysis surface wind stresses with the simulated precipitation and wind stresses. The observation shows that the ITCZ migrates from the equator in March (Fig. 3b) to 10°N in August and returns to the equator during winter (Fig. 3h). This seasonal transition of the ITCZ is well captured by the model, although the phase of the annual cycle in the model during the boreal spring tends to lag the observation by about 1 month, owing to the delay in SST annual cycle. Over West Africa, the rainy season starts in late spring or early summer (May–June), which marks the onset of the West African monsoon. During these months, the maximum precipitation is located along the upper Guinea coast (Fig. 3d). As the season progresses, the maximum precipitation band moves northward to around 10°N at the peak of the monsoon during late boreal summer (August–September) (Fig. 3f). This seasonal variation of the monsoon rainfall over West Africa is also reproduced reasonably well by the model. Overall, the simulated tropical Atlantic mean climate is acceptable for use for further sensitivity experiments.

4. Impact of AMOC changes on TAV

In this section, we will first explore mechanisms through which the AMOC's influence transmits to the tropical Atlantic and then assess the impact of the AMOC on tropical Atlantic climate. We will begin our discussion with the OAME run where both the oceanic and atmospheric forcings are included in the simulation. We will show that the tropical Atlantic response in the OAME run resembles that of water-hosing experiments conducted using CGCMs (e.g., Stouffer et al. 2006; Timmermann et al. 2007). We will then compare the result of OAME to the results of the other experiments

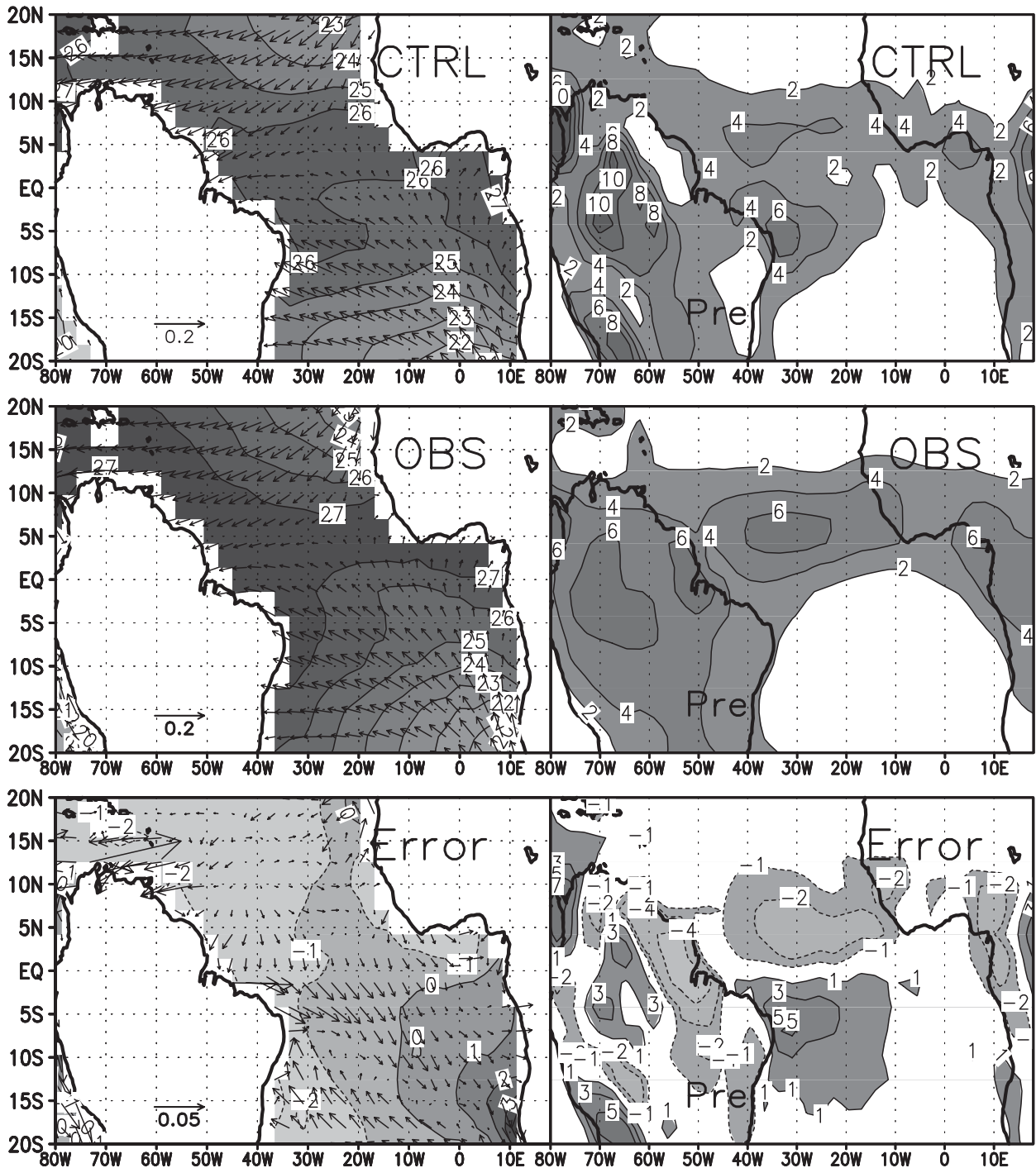


FIG. 1. The annual mean state of the (left) SST ($^{\circ}\text{C}$) and surface wind stress and (right) precipitation: (top) CTRL, (middle) observations, (bottom) the difference between the CTRL run and observations. The vector unit is in N m^{-2} .

to evaluate the relative importance of the oceanic versus atmospheric teleconnection mechanisms. Finally, we will discuss how the changes in the tropical Atlantic SST can have an impact on rainfall variability in the region.

a. Simulated tropical Atlantic response to the collapse of AMOC

Figures 4a and 5a show the simulated ocean temperature and circulation anomalies in the OAME run within

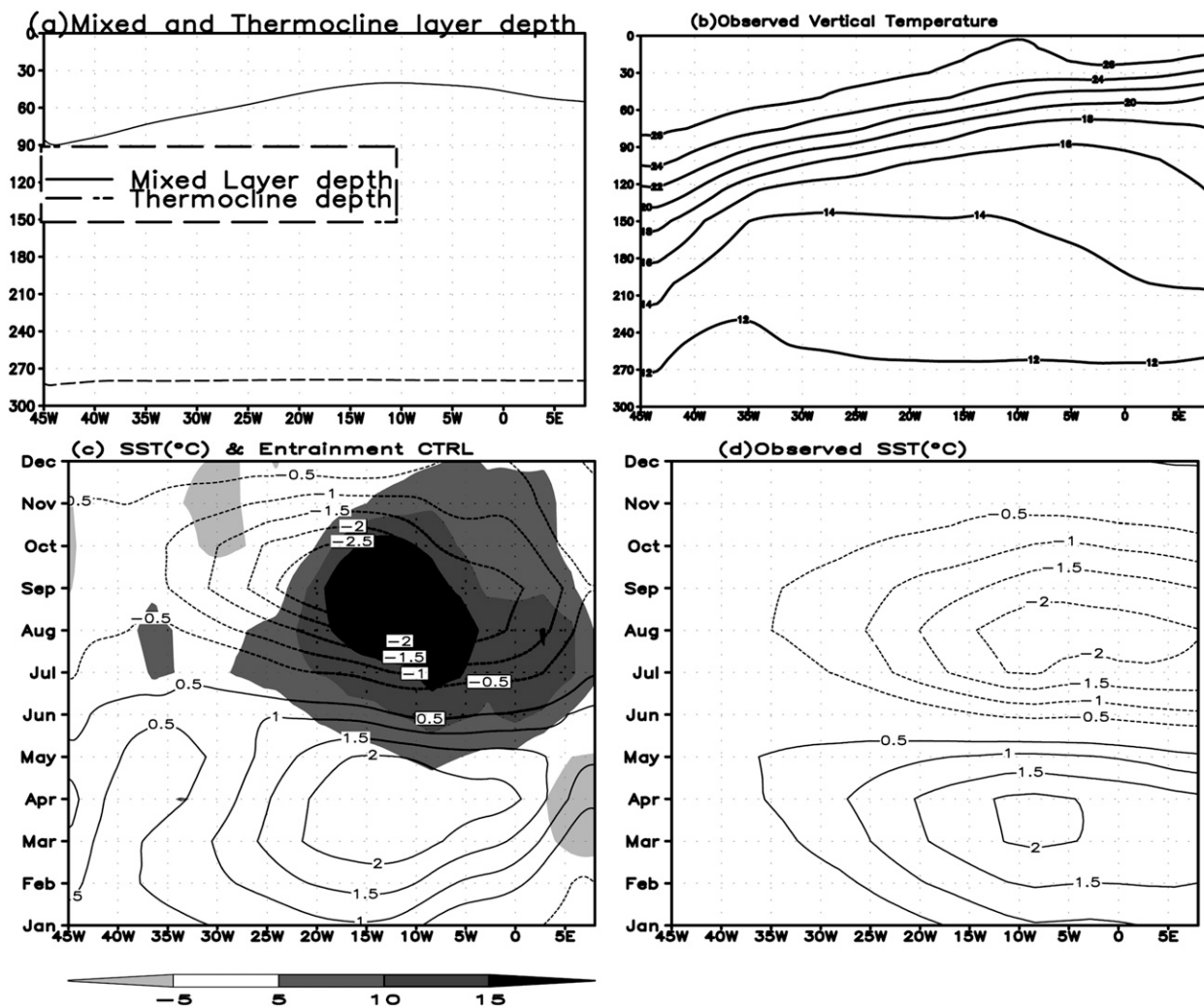


FIG. 2. (a) Annual mean of the mixed layer and the thermocline layer depths along the equator (m). (b) Vertical temperature structure of Levitus dataset (Levitus 1994) along the equator ($^{\circ}\text{C}$). (c) Seasonal cycle of simulated SST (contour, $^{\circ}\text{C}$) and entrainment (shaded, 10^{-6} m s^{-1}) along the equator from the CTRL run. (d) Seasonal cycle of observed SST ($^{\circ}\text{C}$) along the equator (Reynolds et al. 2002).

the mixed layer and the thermocline layer, respectively. Consistent with CGCM water-hosing simulations, an interhemispheric seesaw pattern in the SST response emerges with a strong cooling in excess of 2.5°C in the North Atlantic and a warming on the order of 0.8°C along the equator and along the upwelling zones of the southeastern tropical Atlantic (Fig. 4a). Within the model thermocline layer, a warm temperature anomaly is seen to emanate from the western boundary region off the coast of northern South America, spreading into the deep tropics. The dominant feature of the ocean circulation change is along the western boundary where the current is substantially weakened in the OAME (Fig. 5a). Large-scale circulation response of the atmosphere is also consistent with CGCM water-hosing experiments. The northeasterly trade winds are strengthened in the OAME, while

the southeasterly trades experience little or no changes. Accompanied with the change in the trade winds, the mean position of the ITCZ shifts southward, resulting in a decrease in precipitation rate north of the equator by about 2 mm day^{-1} and an increase south of the equator by about 1.5 mm day^{-1} (Fig. 6a). Over the adjacent continents, there is an increase of precipitation over Northeast Brazil and along the northern coast of the Gulf of Guinea. This change in the atmospheric circulation implies a change in the Hadley Circulation. As shown in Fig. 7a, the imposed AMOC forcing gives rise to enhanced (reduced) upward vertical motion south (north) of the mean ITCZ in the CTRL run, suggesting a southward shift of the Hadley circulation.

The fact that the RCM results agree generally well with the results of fully coupled GCM water-hosing simulations

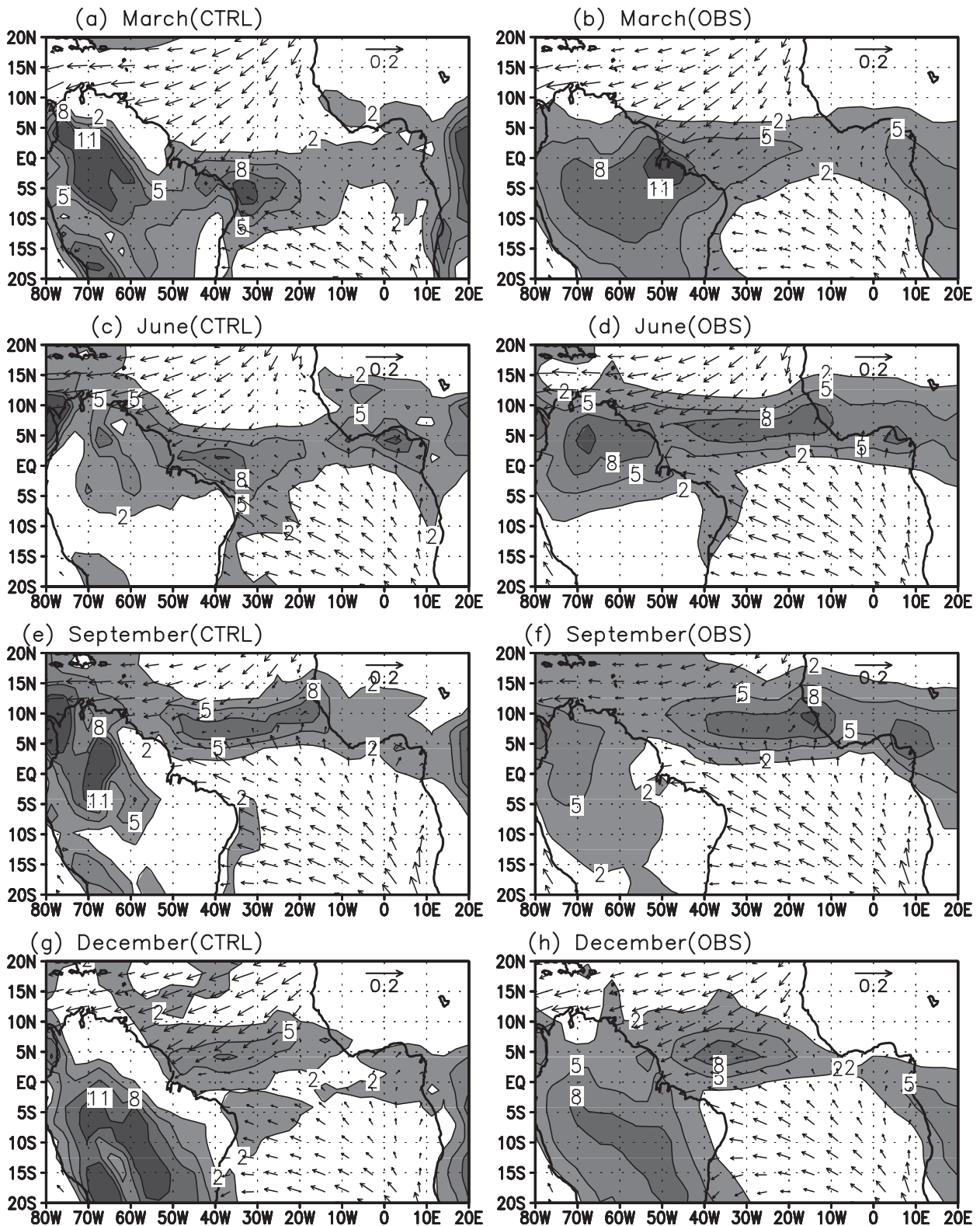


FIG. 3. Annual cycle of precipitation and surface wind stress in (a),(c),(e),(g) the CTRL run and in (b),(d),(f),(h) the GPCP dataset and NCEP reanalysis, respectively. The contour interval of precipitation is 3 mm day^{-1} , starting with 2 mm day^{-1} . The vector unit is N m^{-2} .

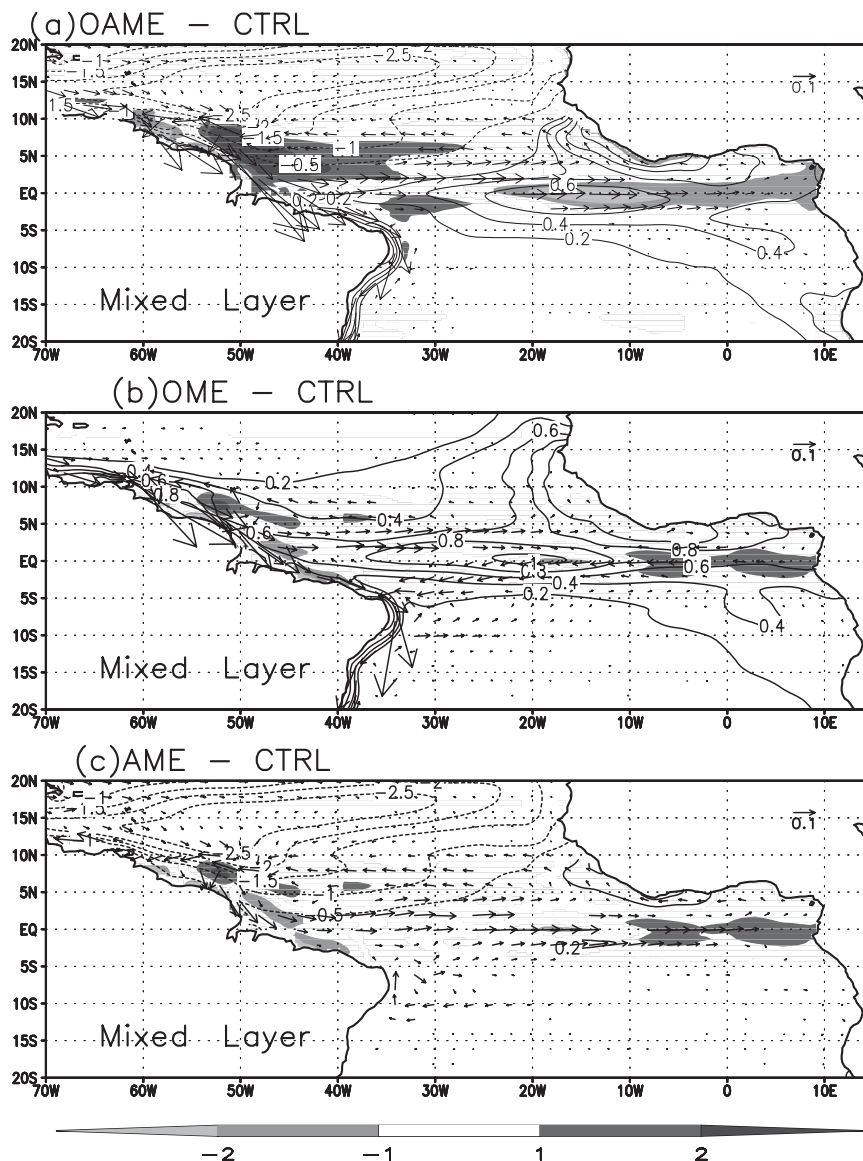


FIG. 4. The SST anomaly (contour, $^{\circ}\text{C}$), velocity anomaly (vectors, m s^{-1}), and entrainment anomaly (shaded, 10^{-6} m s^{-1}) generated in the (a) OAME run, (b) OME run, and (c) AME run in the mixed layer. Plotted values are significant at the 95% statistical significance level using the t test.

(e.g., Stouffer et al. 2006; Timmermann et al. 2007) suggests that the RCM contains the essential oceanic and atmospheric teleconnections linking AMOC changes to tropical Atlantic. However, it is noteworthy that the trade wind response in the south Atlantic simulated by the RCM is generally weaker than that found in many CGCM experiments, suggesting that not all teleconnection mechanisms may be included. Nevertheless, we assess that major features of tropical Atlantic response to AMOC changes are captured and thus proceed with the further examination of the underlying dynamic mechanism.

b. Oceanic versus atmospheric processes

The OAME run reveals that both the ocean circulation change caused directly by a shutdown of the AMOC and the atmosphere circulation change induced by the surface cooling in the North Atlantic contribute to the interhemispheric SST dipole anomaly and the corresponding southward shift of the ITCZ in the tropical Atlantic. In this subsection, we attempt to address the following questions: Is the interhemispheric SST dipole anomaly caused by the oceanic or by the atmospheric

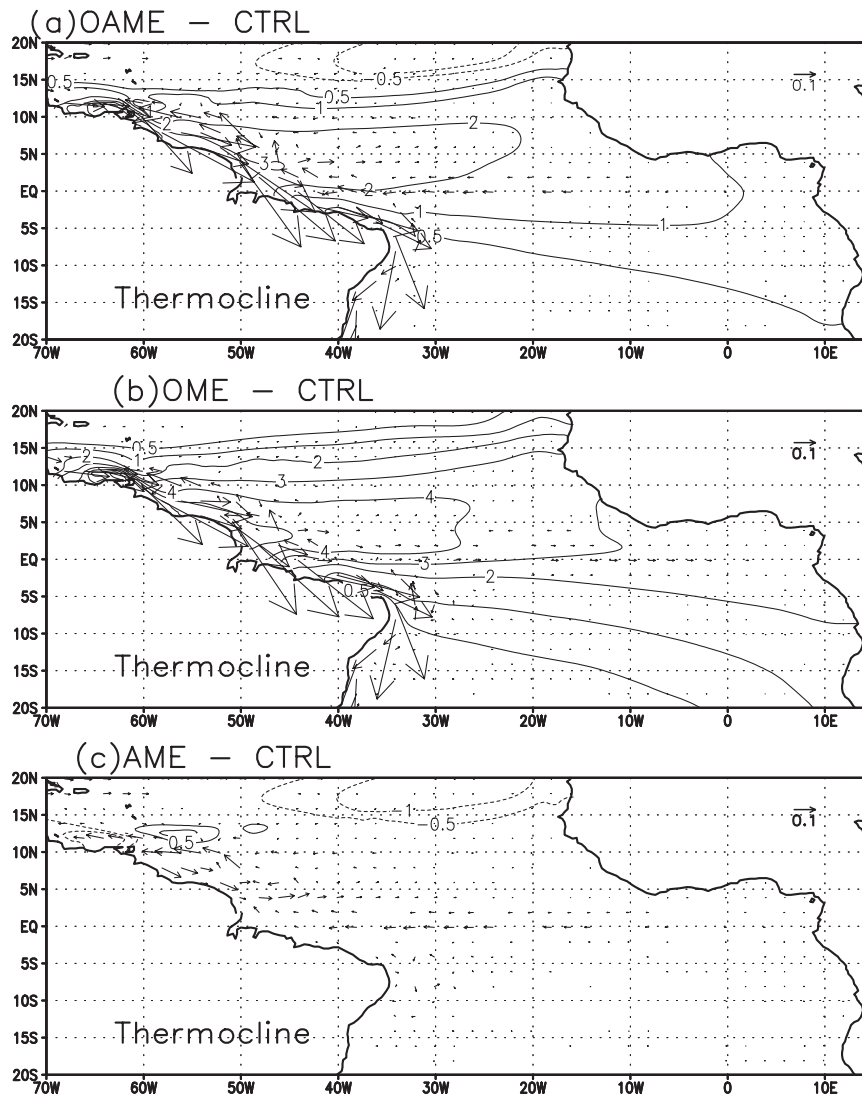


FIG. 5. The annual mean temperature anomaly (contour, $^{\circ}\text{C}$) and velocity anomaly (vectors, m s^{-1}) generated in the (a) OAME run, (b) OME run, and (c) AME run in the thermocline layer. Plotted values are significant at the 95% statistical significance level using the t test.

mechanism? Or is it caused by both? Which of the mechanisms is, or are both responsible for the southward displacement of ITCZ?

To answer these questions, we first turn to the OME run where the response in the tropical Atlantic can only be attributed to the ocean circulation change caused directly by the shutdown of the AMOC because the surface cooling in the North Atlantic is absent. As shown in Fig. 4b and Fig. 5b, the coupled model response is similar to that of ocean-alone discussed in W10, where similar experiments were conducted using the RGO model. The most salient circulation change in response to the shutdown of the AMOC occurs in vicinity of the western boundary. Accompanied with the circulation change, a

pronounced subsurface warming takes place along the western boundary off the coast of northern South America and spreads into the deep tropics. Without the influence of cooling in the North Atlantic, the subsurface warming in the OME run is stronger than that in the OAME run.

Similar to the ocean-alone experiment discussed in W10, the removal of the interhemispheric flow in the model causes the NBC that carries much of the AMOC return flow (Fratantoni et al. 2000) to reverse its direction from north to south. This change of circulation has two major effects on the tropical Atlantic thermocline water: 1) it produces a strong subsurface warming by anomalous heat advection in the region where the strong temperature front between the subtropical and tropical gyres intersects

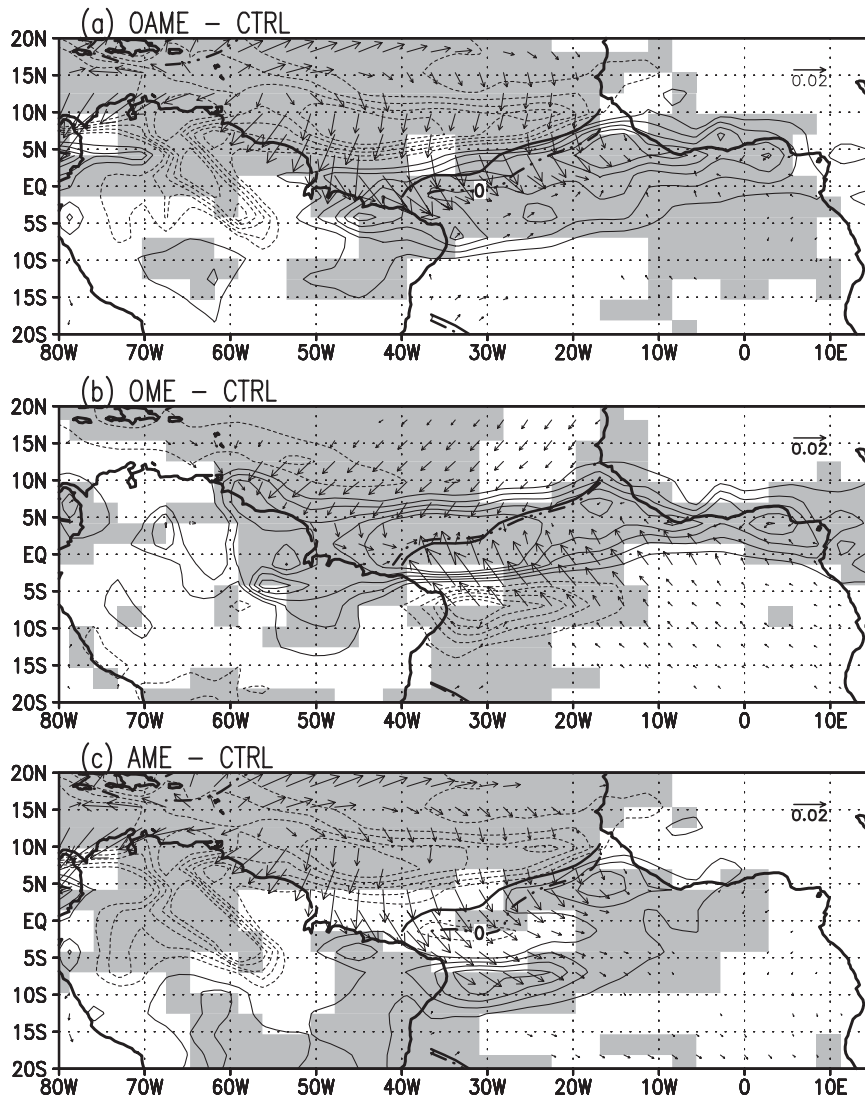


FIG. 6. The annual mean precipitation anomaly (contours, mm day^{-1}) and surface wind stress anomaly (vectors, N m^{-2}) generated in the (a) OAME run, (b) OME run, and (c) AME run. The thick solid line and dot-dash lines represent the annual mean $\tau_v = 0$ lines in the CTRL run and experiment, respectively. For wind stress anomaly, only values exceeding the 95% statistical significance are drawn. For precipitation anomaly, shaded area exceeds the 95% significance level using a t test.

the western boundary; and 2) it changes the pathway of the northern STC by allowing the warm northern subtropical gyre water to enter the equatorial region, causing warming in the equatorial thermocline. This subsurface warming gives rise to surface warming in the entire tropical Atlantic with strong warming along the African coast, near the equator in the central Atlantic, and along the northern coast of north Brazil, where upwelling is strong (Fig. 4b). It indicates that the changes in ocean circulation alone do not produce a dipole-like SST anomaly, instead they give rise a warming in the entire tropical Atlantic.

The atmospheric response to this basinwide warming is different from that in the OAME. The basinwide warming over the tropical Atlantic mainly enhances the Hadley circulation (Fig. 7b), while displacing the maximum vertical velocity slightly southward. Instead of a positive and a negative vertical velocity anomaly that straddle the center of upward motion of the mean Hadley circulation in the OAME (Fig. 7a), the anomalous vertical velocity in the OME run has a single core situated just south of the center of upward motion (Fig. 7b). The enhanced Hadley circulation results in an anomalous convergence just north of the

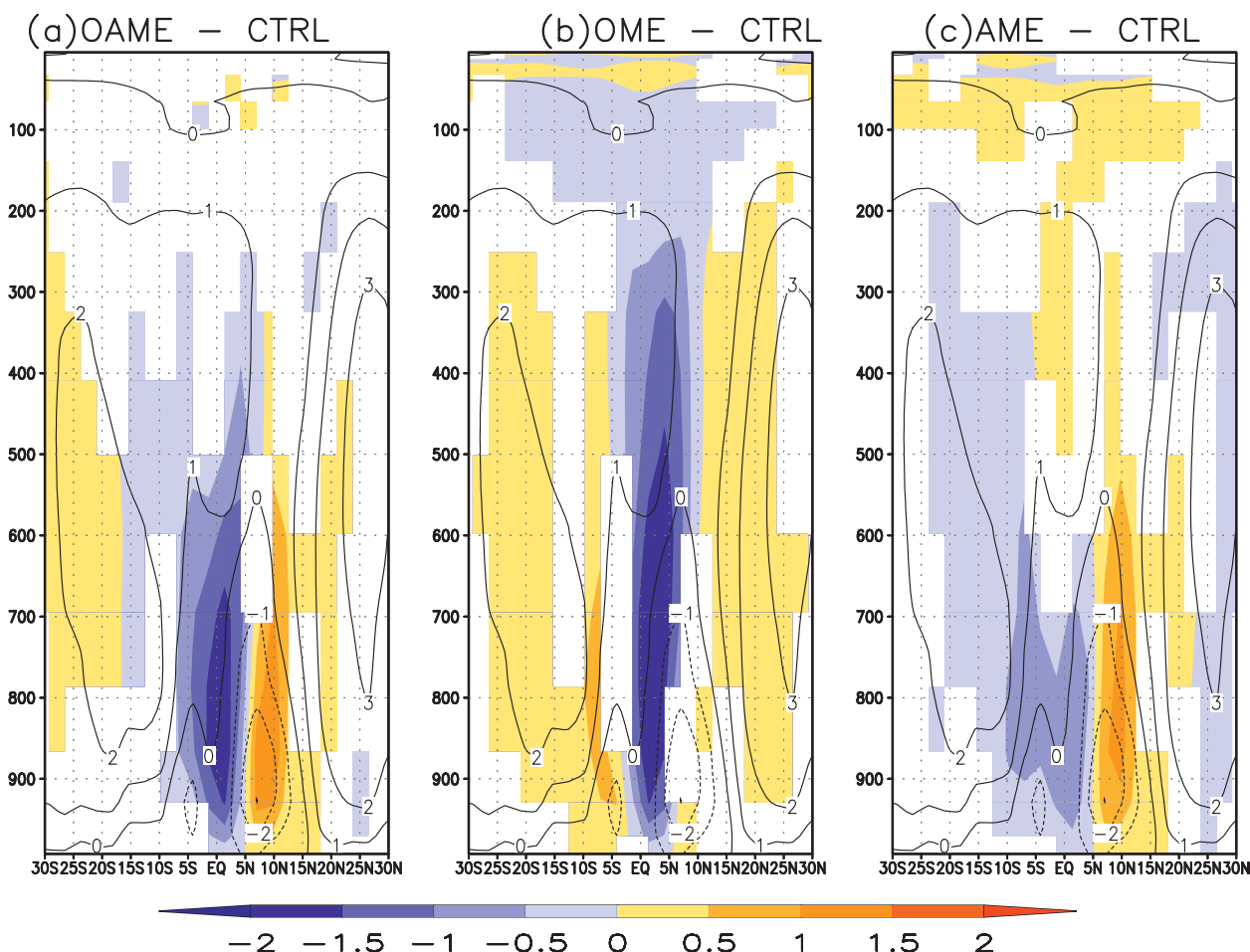


FIG. 7. Anomalous pressure vertical velocity (colors, hPa s^{-1}) averaged over 50°W – 10°E in the (a) OAME run, (b) OME run, and (c) AME run. Contour line: CTRL run. Negative values indicate upward motion. The shaded area exceeds the 95% statistical significance level using the t test.

equator, which in turn enhances the trade winds in the deep tropics. Figure 6b shows clearly a positive precipitation anomaly along the mean convergence zone accompanied by two weak negative anomalies off the equator.

W10 showed that a shutdown of the AMOC also induces a basinwide surface warming in the tropical Atlantic in the ocean-only experiment, while the warming is much weaker than that in the OME with SST anomaly greater than 0.6°C only occurring on the central equatorial region (Fig. 4 of W10). It suggests that SST anomalies resulting from ocean circulation change could be amplified by air–sea interactions. Our analysis suggests that the stronger SST response in the coupled model could be attributed to the local air–sea feedbacks involving the upwelling process. In the ocean-alone experiment, the SST warming is primarily due to the reduction of the mean upwelling acting on the vertical temperature gradient $[\bar{w}(\partial T'/\partial Z)]$ and the anomalous upwelling $[\omega'(\partial \bar{T}/\partial Z)]$ (Fig. 8, bottom panel). In the coupled model, the wind stress anomaly in response to the

surface warming gives rise to a reduction of the upwelling rate in the central equatorial region, the Guinea dome, and the region along the coast of north Brazil (Fig. 8, upper panel), which in turn amplifies the development of the warming anomalies, much in line with the Ekman feedback discussed by Chang and Philander (1994).

In contrast to the OME run, the AME run produced a strong surface cooling in the North Atlantic but only a very weak surface warming in the tropical South Atlantic (Fig. 4c). To the north of 10°N , the cooling is a direct response to the imposed anomalous surface heat flux. South of it, the cooling is likely a result of the WES feedback where intensification of the northeasterly trades causes an increase in latent heat flux that drives the cold SST anomaly equatorward. In response to the surface cooling, the ITCZ moves southward with strengthened northeasterly (weakened southeasterly) trades (Fig. 6c). These features appear generally consistent with the WES feedback, which involves interactions between the SST

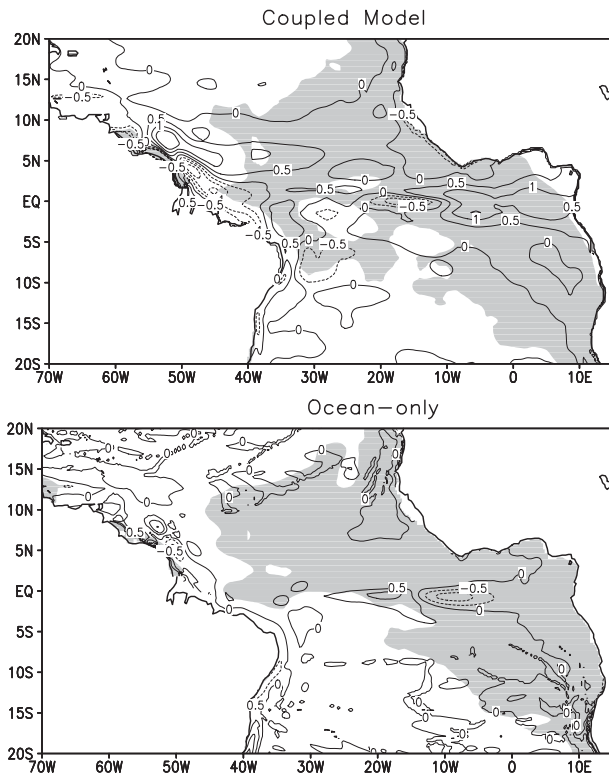


FIG. 8. Comparison of entrainment response to a shutdown of AMOC (contours, 10^{-6} m s^{-1}) in (top) the OME run and (bottom) the ocean-alone experiment (L10NG7C_0Sv run in W10). The shaded areas are positive annual mean entrainment rate of each control run (10^{-6} m s^{-1}).

and wind-induced latent heat flux (Xie and Philander 1994; Chang et al. 1997).

A comparison of the OAME, OME, and AME runs reveals that ocean circulation change is responsible for the surface warming near and to the south of the equator, while the atmospheric processes contribute to the cooling in the northern tropical Atlantic and play only a minor role in the development of surface warming on and south of the equator. Our results indicate that, in terms of the annual mean state, the SST response can be well approximated by a linear superimposition of the responses induced by the oceanic and the atmospheric processes. However, this is not the case for the precipitation response. In the AME run, the southward shift of the ITCZ induces an increase in the annual mean rainfall over Northeast Brazil by $\sim 1.6 \text{ mm day}^{-1}$ (Fig. 6c). The oceanic mechanism causes a decrease in precipitation over the same region by as much as 2.5 mm day^{-1} (Fig. 6b). A linear superimposition of the two would yield a net decrease in the annual mean rainfall in this region. But the OAME produced a positive rainfall anomaly, indicating that precipitation responds nonlinearly.

The competing and complementary influences of atmospheric and oceanic teleconnections on the tropical Atlantic response are also clearly seen during the transient state. To filter out the variability internal to the coupled system, we carried out three ensembles of runs with identical forcing of OAME, OME, and AME, respectively. Each ensemble consists of five 30-yr integrations. The five ensemble members are initialized with slightly different conditions in the AGCM. An average across all ensemble members acts to reduce the effect of internal variability that may make it difficult to identify the coupled model response to the external forcings.

Figure 9 depicts the evolutions of zonally averaged SST and atmospheric response in the OAME, OME, and AME ensemble runs. In the AME (Fig. 9c), the North Atlantic cooling is immediately transmitted toward the equator and reaches an equilibrium state within the first year. The response in the Southern Hemisphere is very weak. Associated with the surface cooling is the c-shaped cross-equatorial surface wind anomaly. The wind anomaly follows the cooling closely and quickly reaches equilibrium within a couple of years. Our result supports the CB05 result that the WES feedback is effective in transmitting cooling toward the equator. In the OME, the positive SST anomaly centered at (0° – 5° N) takes a longer time to develop and reaches a full equilibrium state after 8 years (Fig. 9b). It is evident that the surface warming has a subsurface origin (Fig. 5b). Similar with the ocean-alone experiment discussed in W10, the circulation change along the western boundary triggers the rapid buildup of the subsurface temperature near the strong temperature front. The warm anomaly is then carried equatorward along the western boundary by the reversed NBC. Once the warm anomaly enters the equatorial zone, it is then carried eastward by the Equatorial Undercurrent (EUC). In the OAME, the coupled system response is driven by the fast atmosphere processes and the relatively slow oceanic processes (Fig. 9a). The cooling in the North Atlantic and the wind anomaly rapidly develop within the first couple years. The warm SST anomalies at and to the south of the equator, however, take approximately 8 years to fully develop. This further demonstrates that the oceanic teleconnection is the dominant factor controlling the warming to the south of the equator as discussed above.

c. Impact of AMOC change on the seasonal cycle

In section 4a, it is shown that the AMOC change significantly affects the climatological mean state of the tropical Atlantic. A question immediately arises: does the tropical Atlantic response exhibit any seasonal dependence? In this subsection, we will discuss the impact of the AMOC change on the seasonal cycle of tropical Atlantic. To facilitate the analysis of the coupled response, we

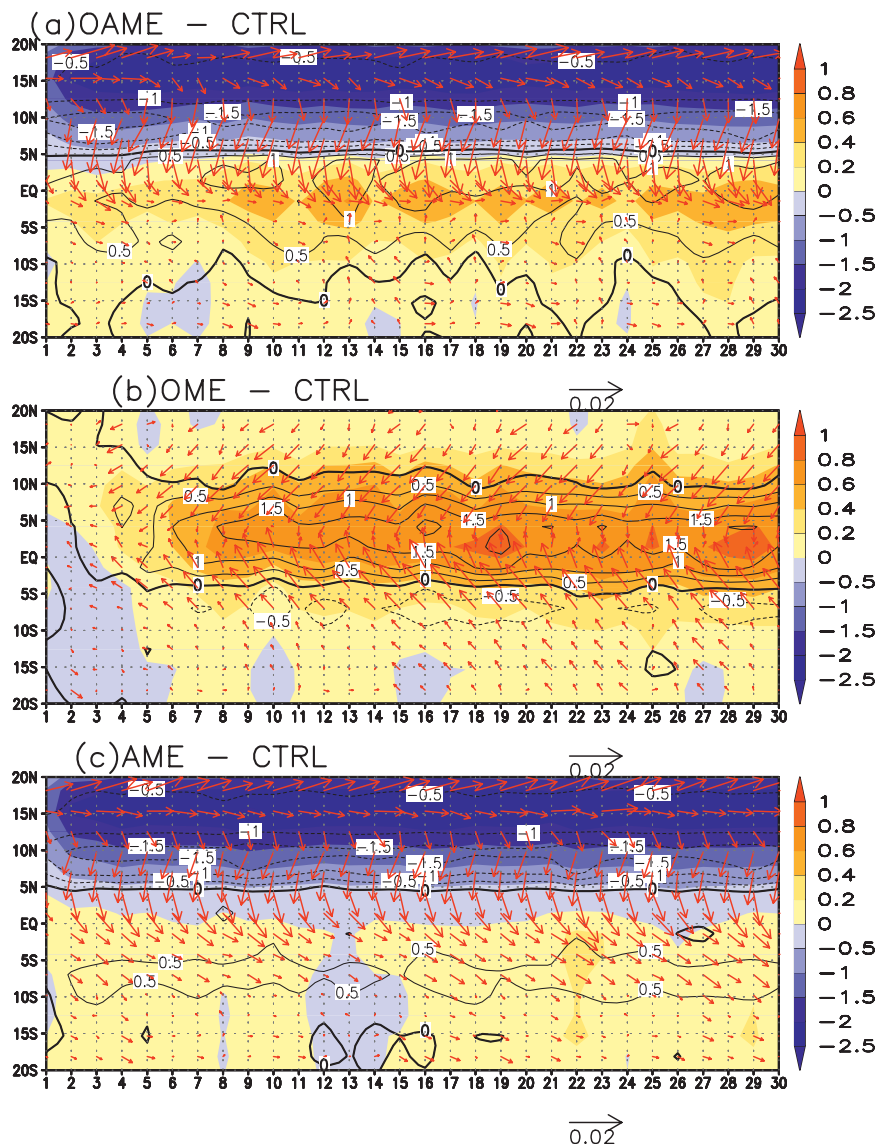


FIG. 9. Time evolution of zonal-averaged SST anomaly (colors, $^{\circ}\text{C}$), wind stress anomaly (vectors, N m^{-2}) and precipitation anomaly (contours, mm day^{-1}) in a 5-member ensemble of the (a) OAME run, (b) OME run, and (c) AME run. All variables are zonally averaged over (60°W – 20°E). The anomaly is defined as the difference between the ensemble mean and the CTRL run.

isolate the atmospheric and oceanic processes via comparison among the OAME, OME, and AME runs as discussed above.

In agreement with other coupled GCM water-hosing experiments (e.g., Timmermann et al. 2007), our results show a marked seasonal cycle of tropical Atlantic SST response to the AMOC change. The strongest surface warming of more than 2°C occurs during July–September in the central equatorial Atlantic, whereas the strongest surface cooling of about -1°C occurs during February–May in the western equatorial Atlantic (Fig. 10a). A

comparison among the OAME, OME, and AME reveals that both oceanic and atmospheric processes contribute to this seasonality. As shown in Fig. 10b, the equatorial SST warming in the OME persists year around and peaks in boreal summer. The warming is mainly forced by the mean upwelling acting on the reduced vertical temperature gradient $[\overline{\omega}(\partial T'/\partial Z)]$ and the reduction of upwelling $[\omega'(\partial \overline{T}/\partial Z)]$ as a result of the deepening of the mixed layer. Both these terms are most effective during boreal summer and fall when upwelling at its peak (Fig. 2c). In the AME, the southeasterly trade

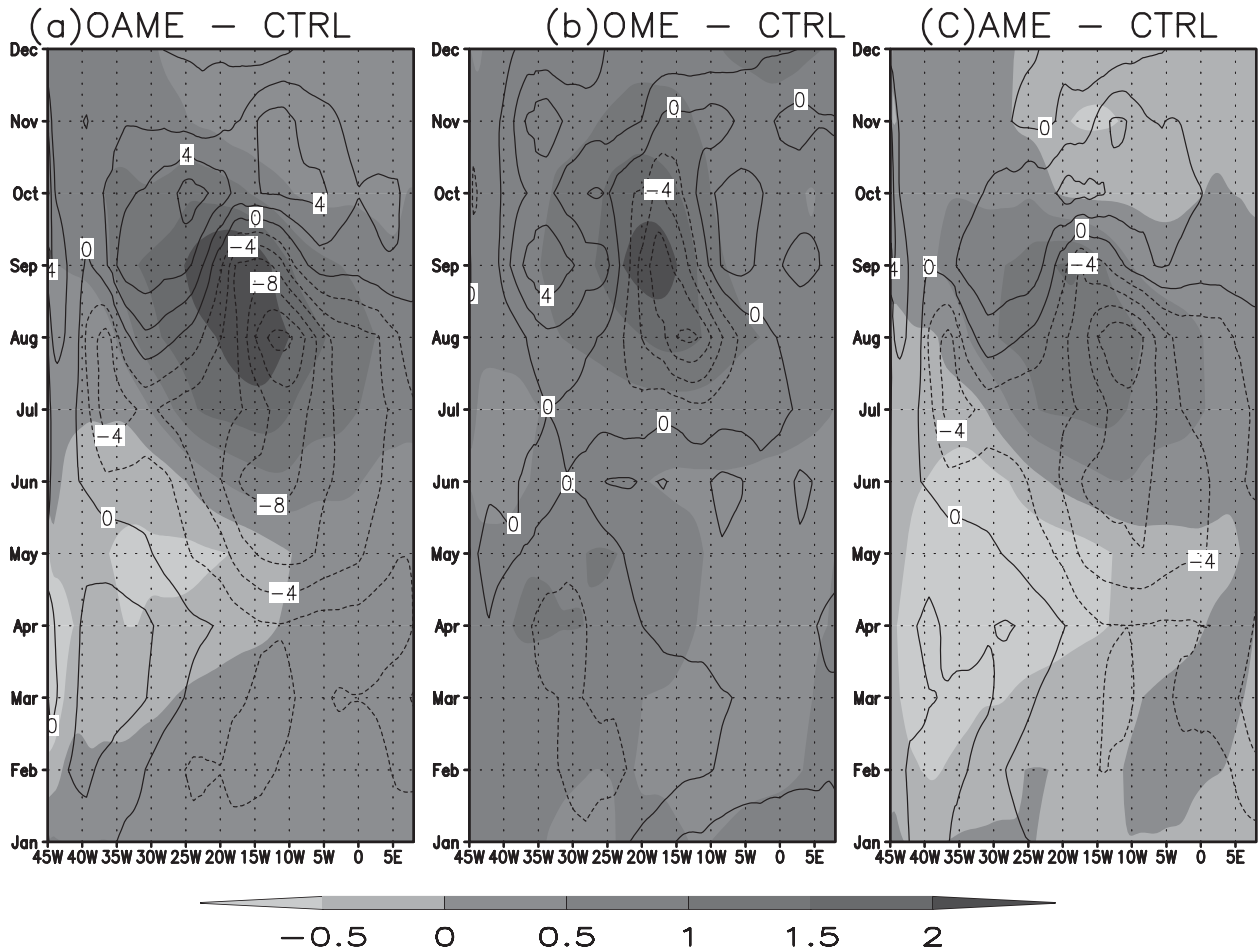


FIG. 10. Annual cycle of SST anomaly (shaded, $^{\circ}\text{C}$) and entrainment anomaly (contours, 10^{-6} m s^{-1}) along the equator in (a) OAME, (b) OME, and (c) AME. Contour interval is $2 \times 10^{-6} \text{ m s}^{-1}$.

winds over the equatorial Atlantic gets weakened from May to July and gets strengthened during the rest of year (not shown). As a result, the entrainment rate is substantially weakened during summer while it is enhanced during fall–winter, leading to warming in boreal summer and cooling in winter (Fig. 10c). Our results point to an important role of the oceanic process in causing the strong anomalous warming in summer. On the other hand, the influence of atmospheric processes is twofold: 1) enhancing the summer warming through reducing upwelling and 2) weakening the warm anomalies during fall–winter.

As shown in section 4a, the precipitation response over the continents adjacent to the AMOC change is most significant over Northeast Brazil and along the upper Guinea coast. To evaluate the seasonality of this response, we define the following indices: 1) Northeast Brazil rainfall index (NEB), which is defined as the precipitation change averaged over the region between

42° – 35°W and 12° – 4°S ; and 2) the Gulf of Guinea rainfall index (GGN), which is defined as the precipitation change averaged over the region between 10°W – 10°E and 0° – 7°N . Both GGN and NEB show a well-defined seasonal cycle in the CTRL run (Fig. 11, black bars). The pronounced seasonal variations in the precipitation over these regions are associated with the seasonal migration of the ITCZ. During spring, the ITCZ approaches its southernmost position and causes more rain in Northeast Brazil. As the ITCZ migrates northward, Northeast Brazil begins its dry season, while the upper Guinea coast enters its rainy season. The simulated annual cycles of these regions are in a reasonable agreement with observations, except that the phase of the precipitation change lags the observation by about 1 month and a semiannual cycle present in the observation is absent in the model over the Gulf of Guinea (Fig. 11, gray bars).

In the OAME, the precipitation over the upper Guinea coast increases over the entire year, which is in

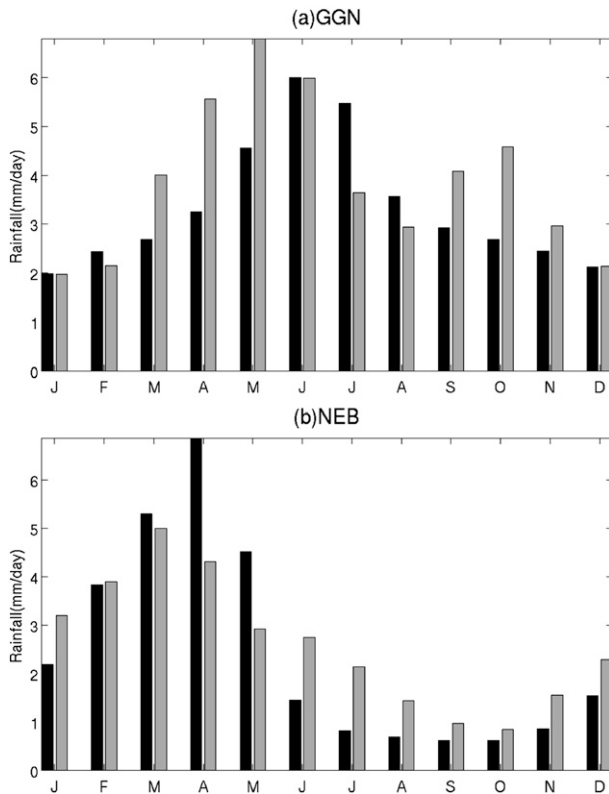


FIG. 11. Seasonal cycle of (top) GGN index and (bottom) NEB index from the CTRL run (black bars) and GPCP dataset (gray bars). GGN index is defined as precipitation averaged over the Gulf of Guinea (10°W – 10°E , 0° – 7°N). NEB index is defined as precipitation averaged over Northeast Brazil (42° – 35°W , 12° – 4°S).

response to the AMOC change with a strong seasonal variation. The precipitation change from January to June is in the range of 0.5 – 1.0 mm day^{-1} , but it increases drastically in July to 2 mm day^{-1} (Fig. 12, top panel). As shown in Fig. 11, the onset date of the West African monsoon in the model occurs around June, the rapid change of precipitation response indicates a change in monsoon circulation. Our analysis suggests that the oceanic and atmospheric processes interact in a complex manner to produce the rainfall response over the Gulf of Guinea. The surface warming produced by the ocean circulation change alone generally gives rise to a positive rainfall anomaly throughout the year and it also gives rise to a semiannual response with the first maximum in May and the second in November. Arguments used to explain the equatorial annual cycle of the Pacific and the Atlantic Oceans may offer one possible explanation of this semiannual response. Li and Philander (Li and Philander 1996) and other studies suggest that air–sea interactions are one of the major factors contributing to the maintenance of the cold-tongue–ITCZ complex in the eastern equatorial Pacific and Atlantic and the

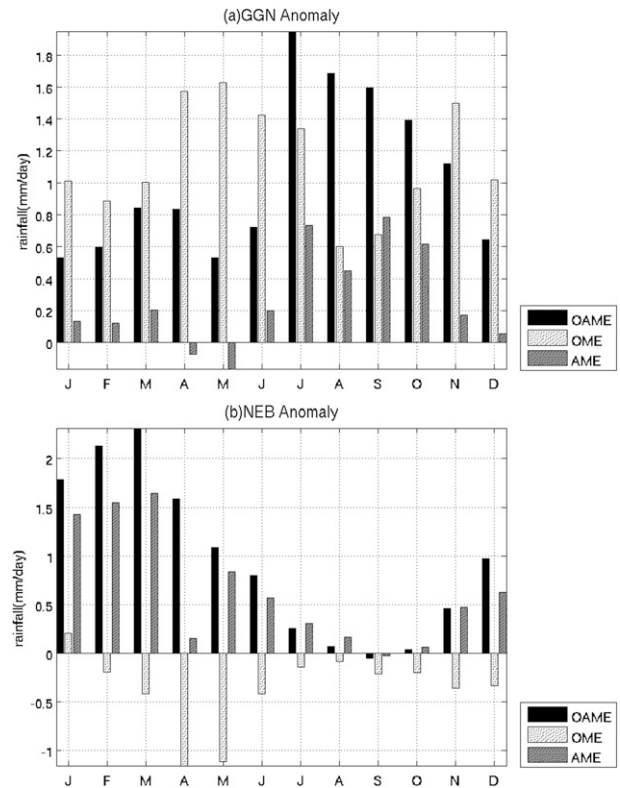


FIG. 12. Seasonal cycle of the rainfall anomaly of (a) GGN index and (b) NEB index in the OAME, OME, AME runs. The definitions of GGN index and NEB index are the same as those in Fig. 11.

pronounced equatorial annual cycle. If the cold tongue disappears, the air–sea interactions will be weakened and the response of the coupled system to seasonal change in solar radiation will behave in a manner similar to that of the Pacific warm pool region, which is dominated by a semiannual cycle of the ITCZ movement near the equator because of the semiannual cycle of solar radiation over the equator. In the AME, the precipitation change in the region is generally small except for the months from July to October. The precipitation response in this case may be due to the fact that during the summer and fall, the cooling in the northern tropical Atlantic makes it difficult for the ITCZ to move northward. As a result, more precipitation occurs over the Gulf of Guinea. Overall, the oceanic process appears to have a stronger influence on the precipitation change in this region. However, the strong rainfall response from July to October in the OAME clearly requires both the oceanic and atmospheric processes.

In contrast to the precipitation change over the Gulf of Guinea, the atmospheric and oceanic processes act as two competing influences over Northeast Brazil. In the OAME, the wet season during boreal spring becomes significantly wetter with little change during the dry season

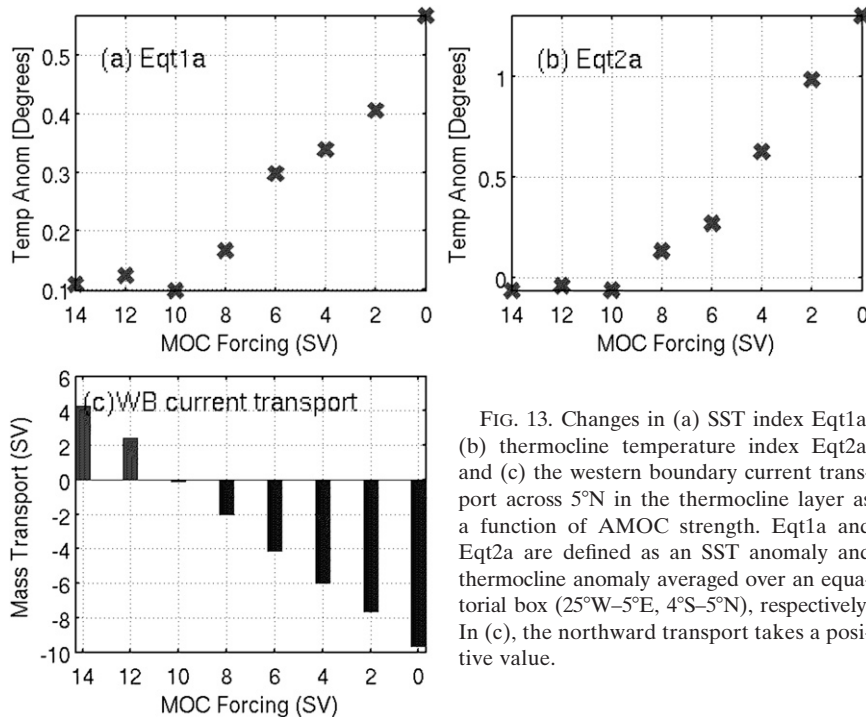


FIG. 13. Changes in (a) SST index Eq1a, (b) thermocline temperature index Eq2a, and (c) the western boundary current transport across 5°N in the thermocline layer as a function of AMOC strength. Eq1a and Eq2a are defined as an SST anomaly and thermocline anomaly averaged over an equatorial box (25°W – 5°E , 4°S – 5°N), respectively. In (c), the northward transport takes a positive value.

(Fig. 12, bottom panel). A comparison between the OME and AME suggests that the atmospheric processes generally tend to increase the precipitation, whereas the oceanic processes tend to reduce the precipitation. Our results suggest that precipitation changes over Northeast Brazil are primarily attributed to the atmospheric processes. Note that the total precipitation change in the OAME cannot be simply explained as a linear superposition of precipitation changes in the OME and AME as SST changes discussed above.

5. Sensitivity of tropical Atlantic response to changes in AMOC strength

It is demonstrated in W10 that the equatorial SST responds nonlinearly to changes in AMOC strength in ocean-alone experiments. A prominent equatorial warming occurs when AMOC is weakened below a threshold value. In this section, we will examine whether similar nonlinear behavior also exists in the coupled system and explore how it is manifested in the atmosphere.

For this purpose, we performed a set of coupled simulations, where the forcing configurations are the same as those in the OAME except that the imposed northward mass transport at the open boundary is decreased systematically from 14 to 0 Sv. The CTRL run with the imposed 14-Sv interhemispheric flow serves as a reference for all sensitive experiments.

Similar to the ocean-only experiment, we define two temperature indices to assess the SST response sensitivity. Eq1a is defined as the SST from each experiment averaged over an equatorial box of 25°W – 5°E and 4°S – 5°N and then subtracted by the SST from the control run; Eq2a is the same as Eq1a except that it is taken from the thermocline layer. Figure 13 shows these indices as a function of AMOC strength. Evidently, both Eq1a and Eq2a exhibit nonlinear behavior. The rate of equatorial temperature change increases rapidly when AMOC decreases below 10 Sv. This nonlinear behavior holds for all seasons (not shown). As pointed out in W10, the nonlinear SST response over the equatorial zone is associated with the interplay between the wind-driven northern STC and the AMOC. Figures 4 and 5 show that the return flow of the AMOC mainly interacts with the wind-driven circulation via western boundary currents (Fontaine et al. 1999; Fratantoni et al. 2000; W10). In the presence of a strong AMOC, the NBC of the Southern Hemisphere origin penetrates into the Northern Hemisphere and effectively blocks the return branch of the northern STC. As the AMOC weakens, the strength of the northward western boundary current decreases. When the imposed AMOC strength is below 10 Sv, the equatorward branch of the northern STC overpowers the AMOC current, causing the NBC to reverse its direction (Fig. 13c). As a result, the subsurface temperature anomaly near the subsurface thermal front generated by

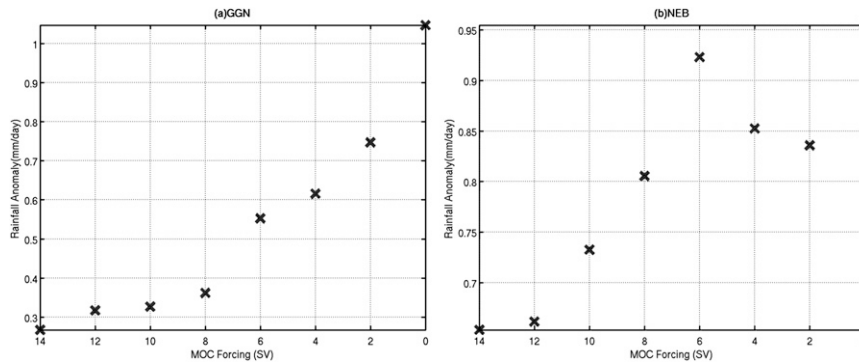


FIG. 14. Changes in (a) GGN index and (b) NEB index as a function of AMOC strength. The definitions of GGN and NEB indices are the same as those in Fig. 11.

AMOC changes is able to enter the equator zone and propagates eastward along the equatorial zone. This in turn leads to the substantial equatorial warming.

The response of the SST in the coupled model differs somewhat from that in the ocean-alone simulation in W10 in the sense that the threshold of the AMOC reduction is lower in the coupled model (10 Sv) than that in the ocean-alone simulation (8 Sv, Fig. 8c in W10). Using the same mass transport analysis in W10, we measure the strength of northern STC by the zonally integrated annual mean meridional circulation at 8°N in the experiment where AMOC is set to 0 Sv and the ocean circulation is wind-driven only. By this measurement, the northern STC in the coupled system is 8 Sv, which is 30% stronger than that (6 Sv) estimated in the uncoupled model (W10). As a result, the NBC in the thermocline layer reverses its direction from northward to southward when the AMOC strength is below 10 Sv, instead of 8 Sv in the ocean-alone simulation (Fig. 8c in W10). It is then easier for the warm subsurface anomaly to propagate into the equatorial zone, resulting in a lower threshold for the nonlinear SST response behavior in the coupled model. As shown in Fig. 6c, the stronger northern STC probably results from the enhanced northeasterly trade winds in response to the cooling over the North Atlantic. This suggests that the lower threshold for the AMOC reduction in the coupled model is likely attributed to the influence of air–sea interactions.

Does the precipitation response show a similar behavior? We assess the sensitivity of precipitation response along the upper Guinea coast and over Northeast Brazil using the GGN and NEB index. Similar with SST response (Fig. 13a), the precipitation response along the upper Guinea coast also shows a clear nonlinear response (Fig. 14a). This result is consistent with C08 who reported a rapid regime shift in the West African monsoon in response to a substantial weakening in the AMOC. In contrast, the relation between the precipitation response

and AMOC changes over Northeast Brazil is ambiguous (Fig. 14b). The different behaviors over the Gulf of Guinea and Northeast Brazil can again be attributed to the different contribution of the atmospheric and oceanic processes in these two regions. As shown in section 4c, the oceanic processes play an important role in affecting precipitation response over the Gulf of Guinea. As a result, sensitivity of precipitation response follows the behavior of the SST response, which is nonlinear. On the contrary, the precipitation response over Northeast Brazil is controlled by the atmospheric processes, which do not display a threshold behavior. It should be noted that our results are based on a single simulation, so some of the complex behavior in NEB rainfall response may be due to contamination of internal atmospheric variability.

6. Conclusions

In this study, we investigate the impact of AMOC changes on tropical Atlantic climate in the framework of a RCM consisting of an AGCM (CCM3) coupled to a tropical Atlantic RGO model. We demonstrate that the RCM is capable of simulating many key features of both mean climate and climate variability in the tropical Atlantic sector and presents perhaps one of the simplest coupled climate models that can be used to explore the underlying dynamical processes linking AMOC changes to TAV.

We conduct extensive numerical experiments with the RCM to examine the relative importance of oceanic versus atmospheric processes in linking AMOC changes to the tropics. We find that ocean circulation changes directly induced by AMOC changes and atmosphere circulation changes driven by surface cooling in the North Atlantic work in concert to generate the dipole-like SST pattern and a southward shift of the ITCZ. From a set of sensitivity experiments, we identify that the oceanic mechanism is the primary factor contributing to the warming near and to the south of the equator and much of the precipitation

changes over the Gulf of Guinea. When the AMOC is absent, the NBC flows equatorward and the STCs become more symmetric about the equator. These circulation changes cause a significant subsurface warming, which leads to surface warming in the Gulf of Guinea and along the African coast. This finding supports the hypothesis proposed by C08. Meanwhile, a reduction of entrainment induced by weakened southeasterly trade wind enhances the surface warming on the equator. On the other hand, the atmospheric processes are largely responsible for establishing the surface cooling in the tropical North Atlantic and the southward displacement of ITCZ, lending support to CB05.

The response of tropical Atlantic to AMOC changes exhibits a pronounced seasonality. The surface warming is strongest during the boreal summer and fall when the seasonal equatorial upwelling is at its peak. Both the reduced vertical temperature gradient and weakened entrainment contribute the surface warming during these seasons. A seasonal preference is also shown in the precipitation response. AMOC changes can lead to excessive rainfall over Northeast Brazil with a peak during spring and along the upper Guinea coast with a peak during boreal summer. The seasonal precipitation response over Northeast Brazil is consistent with the southward shift of the ITCZ, suggesting the importance of atmospheric processes. Along the upper Guinea coast, however, the surface warming over the Gulf induced by oceanic processes contributes significantly to both the mean and the seasonal cycle of precipitation change.

To assess the sensitivity of the tropical Atlantic coupled system to changes in AMOC strength, a set of sensitivity experiments is conducted where the imposed northward transport at the open boundaries is systematically decreased from 14 to 0 Sv. We find that the cold-tongue SST responds nonlinearly to AMOC changes. The sensitivity of the SST response to AMOC changes increases rapidly when AMOC strength decreases below a threshold value of about 10 Sv. Such a nonlinear behavior is also found in precipitation change over the Gulf of Guinea. This implies that prominent equatorial warming can only occur during strong climatic events, such as Younger Dryas, when substantial AMOC reductions occurred. The nonlinear behavior is attributed to the reversal of the NBC when the western boundary current carrying AMOC return flow becomes weaker than the northern STC return flow. This behavior, however, is weaker in the coupled system than that in the stand-alone RGO experiments as shown in W10. The reason is that the intensified northeasterly trade winds in response to the surface cooling in the North Atlantic produce a stronger northern STC in the coupled simulation, which lowers the threshold for NBC reversal.

Our results suggest that the SST response in the northern tropical Atlantic to a weakened AMOC is controlled by a set of competing atmospheric and oceanic processes that tend to counteract with each other. The ocean circulation change tends to produce a surface warming, working against the surface cooling brought down to the tropics by atmospheric processes. The competing nature of these processes may give rise to a complex pattern of SST response to AMOC changes in certain areas. For example, the SST off the coast of north Brazil shows a cooling response to a slightly weakened AMOC but a warming response to a substantially weakened AMOC. The competing nature of atmospheric and oceanic processes also manifests itself in precipitation response over the Northeast Brazil.

Using a decoupling technique, Krebs and Timmermann (2007) demonstrated that the cooling of the North Atlantic is attributed to the atmospheric processes involving air–sea coupling and the south Atlantic warming could be mostly explained by the induced oceanic adjustment in response to a slowdown of the AMOC. Within a regional coupled model framework, we found that neither atmospheric processes alone nor the oceanic processes involving the interaction between the AMOC and the STCs alone could explain the Atlantic SST dipole response pattern. Our results therefore support Krebs and Timmermann's findings. Furthermore, our sensitive studies suggest that complex and competing atmosphere–ocean processes are involved in TAV's response to AMOC changes and the nature of the response can vary considerably from one region to another. This complexity should be taken into consideration in Atlantic abrupt climate studies. Our results not only advance our understanding of the role of the AMOC in abrupt climate change but also shed light on the impact of the AMOC on TAV and its predictability. Model results show that equatorial warming lags the AMOC change by about 8 years. This delayed response may give rise to a certain predictability of equatorial SST in response to AMOC changes at decadal time scales. Further studies are needed to explore AMOC-related predictability in the tropical Atlantic sector.

The coupled model described in this study might be the simplest model that is capable of resolving interactions between the return flow of the AMOC and the wind-driven circulation. This simplified coupled model provides an effective tool to study the impact of the AMOC on the tropical Atlantic climate. However, the simplified physics also gives rise to caveats of the model. There are three important caveats that could affect the results of this study. The first is that the salinity effect is neglected in the model. In reality, precipitation and ocean circulation changes can modify the salinity distribution in the ocean,

which in turn may affect SST pattern (e.g., Breugem et al. 2008). The second is that the upper tropical Atlantic is crudely represented by two active layers of uniform initial depth, neglecting the exchange between thermocline water and intermediate water. In the real ocean, the thickness of the thermocline layer will readjust when stratification changes in response to AMOC changes. The third is that an idealized thermal front is prescribed in this simple model. Such simple treatment of the subsurface temperature is unrealistic as it completely ignores the circulation effect associated with the front. More discussion of this issue can be found in W10.

Acknowledgments. We would like to acknowledge three anonymous reviewers for their comments on the manuscript. This work was supported by the DOE Grant DEFG02-08ER64620 and the NOAA Grant NA09OAR4310135. PC also acknowledges the support from the National Basic Research Program (2007CB816005) and National Science Foundation of China (40730843).

REFERENCES

- Breugem, W.-P., W. Hazeleger, and R. J. Haarsma, 2006: Multi-model study of tropical Atlantic variability and change. *Geophys. Res. Lett.*, **33**, L23706, doi:10.1029/2006GL027831.
- , P. Chang, C. J. Jang, J. Mignot, and W. Hazeleger, 2008: Barrier layers and tropical Atlantic SST biases in coupled GCMs. *Tellus*, **60A**, 885–897.
- Broecker, W. S., D. M. Peteet, and D. Rind, 1985: Does the ocean–atmosphere system have more than one stable state of operation? *Nature*, **54**, 21–26.
- Chang, P., and S. G. H. Philander, 1994: A coupled ocean–atmosphere instability of relevance to seasonal cycle. *J. Atmos. Sci.*, **51**, 3627–3648.
- , L. Ji, and H. Li, 1997: A decadal climate variation in the tropical Atlantic Ocean from thermodynamic air–sea interactions. *Nature*, **385**, 516–518.
- , R. Saravanan, L. Ji, and G. C. Hegerl, 2000: The effect of local sea surface temperatures on atmospheric circulation over the tropical Atlantic sector. *J. Climate*, **13**, 2195–2216.
- , and Coauthors, 2008: Oceanic link between abrupt changes in the North Atlantic Ocean and the African monsoon. *Nat. Geosci.*, **1**, 444.
- Chiang, J., and C. M. Bitz, 2005: Influence of high latitude ice cover on the marine intertropical convergence zone. *Climate Dyn.*, **25**, 477–496.
- , W. Cheng, and C. M. Bitz, 2008: Fast teleconnections to the tropical Atlantic sector from Atlantic thermohaline adjustment. *Geophys. Res. Lett.*, **35**, L07704, doi:10.1029/2008GL033292.
- Davey, M. K., and Coauthors, 2002: STOIC: A study of coupled model climatology and variability in tropical ocean regions. *Climate Dyn.*, **18**, 403–420.
- Fontaine, B., S. Janicot, and P. Roucou, 1999: Coupled ocean–atmosphere surface variability and its climate impacts in the tropical Atlantic region. *Climate Dyn.*, **15**, 451–473.
- Fratantoni, D. M., W. E. Johns, T. L. Townsend, and H. E. Hurlburt, 2000: Low-latitude circulation and mass transport pathways in a model of the tropical Atlantic Ocean. *J. Phys. Oceanogr.*, **30**, 1944–1966.
- Haarsma, R. J., E. J. D. Campos, W. Hazeleger, and C. A. Severijns, 2008: Influence of the Meridional overturning circulation on tropical Atlantic climate and variability. *J. Climate*, **21**, 1403–1416.
- Hastenrath, S., 1984: Interannual variability and annual cycle: Mechanisms of circulation and climate in the tropical Atlantic sector. *Mon. Wea. Rev.*, **112**, 1097–1107.
- Haug, G. H., K. A. Hughen, D. M. Sigman, L. C. Peterson, and U. Rohl, 2001: Southward migration of the intertropical convergence zone through the holocene. *Science*, **293**, 1304–1308.
- Hazeleger, W., and R. J. Haarsma, 2005: Sensitivity of tropical Atlantic climate to mixing in a coupled ocean–atmosphere model. *Climate Dyn.*, **25**, 387–399.
- Huffman, G. J., and Coauthors, 1997: The global precipitation climatology project (GPCP) combined precipitation dataset. *Bull. Amer. Meteor. Soc.*, **78**, 5–20.
- Hurrell, J. W., J. J. Hack, B. A. Boville, D. L. Williamson, and J. T. Kiehl, 1998: The dynamical simulation of the NCAR Community Climate Model version 3 (CCM3). *J. Climate*, **11**, 1207–1236.
- Johnson, H. L., and D. P. Marshall, 2002: A theory for the surface Atlantic response to thermohaline variability. *J. Phys. Oceanogr.*, **32**, 1121–1132.
- Kalnay, E., and Coauthors, 1996: The NCEP/NCAR 40-Year Reanalysis Project. *Bull. Amer. Meteor. Soc.*, **77**, 437–471.
- Krebs, U., and A. Timmermann, 2007: Tropical air–sea interactions accelerate the recovery of the Atlantic meridional overturning circulation after a major shutdown. *J. Climate*, **20**, 4940–4956.
- Levitus, S., 1994: *World Ocean Atlas 1994*. U.S. Department of Commerce, 552 pp.
- Li, T., and S. G. H. Philander, 1996: On the annual cycle of the eastern equatorial Pacific. *J. Climate*, **9**, 2986–2998.
- Ma, C.-C., C. R. Mechoso, A. W. Robertson, and A. Arakawa, 1996: Peruvian stratus clouds and the tropical Pacific circulation: A coupled ocean–atmosphere GCM study. *J. Climate*, **9**, 1635–1645.
- Marchesiello, P., J. C. McWilliams, and A. Shchepetkin, 2001: Open boundary conditions for long-term integration of regional oceanic models. *Ocean Modell.*, **3**, 20.
- McCreary, J. P., P. K. Kundu, and R. L. Molinari, 1993: A numerical investigation of dynamics, thermodynamics and mixed-layer processes in the Indian Ocean. *Prog. Oceanogr.*, **31**, 181–244.
- Mitchell, T. P., and J. M. Wallace, 1992: On the annual cycle in equatorial convection and sea surface temperature. *J. Climate*, **5**, 1140–1156.
- Moura, D. A., and J. Shukla, 1981: On the dynamics of droughts in northeast Brazil: Observations, theory and numerical experiments with a general circulation model. *J. Atmos. Sci.*, **38**, 2653–2675.
- Nobre, P., and J. Shukla, 1996: Variations of sea surface temperature, wind stress, and rainfall over the tropical Atlantic and South America. *J. Climate*, **9**, 2464–2479.
- Piotrowski, A. M., S. L. Goldstein, S. R. Hemming, and R. G. Fairbanks, 2005: Temporal relationships of carbon cycling and ocean circulation at glacial boundaries. *Science*, **307**, 1933–1938.
- Reynolds, W. R., N. A. Rayner, T. M. Smoth, D. C. Stokes, and W. Wang, 2002: An improved in situ and satellite SST analysis for climate. *J. Climate*, **15**, 1609–1625.
- Saravanan, R., and P. Chang, 2000: Interaction between tropical Atlantic variability and El Niño–Southern Oscillation. *J. Climate*, **13**, 2177–2194.

- Smith, T. M., R. W. Reynolds, R. E. Livezey, and D. C. Stokes, 1996: Reconstruction of historical sea surface temperatures using empirical orthogonal functions. *J. Climate*, **9**, 1403–1420.
- Stouffer, R. J., and Coauthors, 2006: Investigating the causes of the response of the thermohaline circulation to past and future climate changes. *J. Climate*, **19**, 1365–1387.
- Timmermann, A., and Coauthors, 2007: The influence of a weakening of the Atlantic meridional overturning circulation on ENSO. *J. Climate*, **20**, 4899–4919.
- Wan, X., P. Chang, R. Saravanan, R. Zhang, and M. W. Schmidt, 2009: On the interpretation of Caribbean paleotemperature reconstructions during the Younger Dryas. *Geophys. Res. Lett.*, **36**, L02701, doi:10.1029/2008GL035805.
- Wen, C., P. Chang, and R. Saravanan, 2010: Effect of Atlantic meridional overturning circulation changes on tropical Atlantic sea surface temperature variability: A 2½-layer reduced-gravity ocean model study. *J. Climate*, **23**, 312–332.
- Wu, L., C. Li, C. Yang, and S. P. Xie, 2008: Global teleconnections in response to a shutdown of the Atlantic meridional overturning circulation. *J. Climate*, **21**, 3002–3019.
- Xie, S. P., and S. G. H. Philander, 1994: A coupled ocean–atmosphere model of relevance to the ITCZ in the eastern Pacific. *Tellus*, **46A**, 340–350.
- Yang, J., 1999: A linkage between decadal climate variations in the Labrador Sea and the tropical Atlantic Ocean. *Geophys. Res. Lett.*, **26**, 1023–1026.
- Yu, J.-Y., and C. R. Mechoso, 1999: Links between annual variations of Peruvian stratocumulus clouds and of SSTs in the eastern equatorial Pacific. *J. Climate*, **12**, 3305–3318.
- Zhang, R., 2008: Coherent surface–subsurface fingerprint of the Atlantic meridional overturning circulation. *Geophys. Res. Lett.*, **35**, L20705, doi:10.1029/2008GL035463.
- , and T. L. Delworth, 2005: Simulated tropical response to a substantial weakening of the Atlantic thermohaline circulation. *J. Climate*, **18**, 1853–1860.